Physica B: Condensed Matter

Computational investigation of the effect of metal plasmonic on the hole transport of polymer solar cell

--Manuscript Draft--

Manuscript Number:	PHYSB-D-23-00896
Article Type:	Research Paper
Section/Category:	Condensed Matter Physics
Keywords:	ZnS nano-particle; Charge transport, Photons-harvesting, Organic solar cell
Abstract:	Semiconductor organic solar absorber exhibits poor charge transport process because of exciton short diffusion length, short life time, and poor carrier mobilities in the medium. Such transport properties have negatively impacted the performance of organic solar cells (OSC). This article is designed to investigate the effect of solar absorber thickness and metal plasmonicnanoparticles using the most popular polymer blend (P3HT:PCBM) via SCAPS device simulation program. Bulk hetero-junction (BHJ) design of OSC has partially addressed the challenges by increasing inter facial area of acceptor/donor (A/D) molecular interfaces, which increases the generation of free charges. However, the collection of these charges remain drawback due to small carrier mobilities in polymer medium. Significant influence of the Zinc Sulfide(ZnS) metal nanoparticles(NPs) have been observed on the performance of OSC at various concentrations. Thus, we are reporting here the effect of ZnSNPs on the charge transport process in OSC.

Computational investigation of the effect of metal plasmonic on the hole transport of polymer solar cell

Ncedo Jili[1], Nkosinathi Dlamini[1], Genene Tessema Mola[1*]
[1] *School of Chemistry & Physics, University of KwaZulu-Natal, Pietermaritzburg Campus,Private Bag X01, Scottsville 3209, South Africa*
(Dated: April 20, 2023)

Semiconductor organic solar absorber exhibits poor charge transport process because of exciton short diffusion length, short life time, and poor carrier mobilities in the medium. Such transport properties have negatively impacted the performance of organic solar cells (OSC). This article is designed to investigate the effect of solar absorber thickness and metal plasmonic nanoparticles using the most popular polymer blend (P3HT:PCBM) via SCAPS device simulation program. Bulk hetero-junction (BHJ) design of OSC has partially addressed the challenges by increasing inter facial area of acceptor/donor (A/D) molecular interfaces, which increases the generation of free charges. However, the collection of these charges remain drawback due to small carrier mobilities in polymer medium. Significant influence of the Zinc Sulfide(ZnS) metal nanoparticles(NPs) have been observed on the performance of OSC at various concentrations. Thus, we are reporting here the effect of ZnS NPs on the charge transport process in OSC. These results are discussed and possible mechanisms are presented.

PACS numbers: 73.61.ph; 73.61 Wp

Keywords: ZnS nano-particle; Charge transport, Photons-harvesting, Organic solar cell

I. INTRODUCTION

Semiconductor polymers have attracted numerous research interests because of its application in photonic devices such organic solar cells (OSCs), organic light emitting diode(OLD), organic sensors etc. The market values organic molecules-based device is continuously increasing by the introduction of new technology and applications. This article is trying to address some of the challenges of thin film organic solar cell. Organic solar has been under intense investigations for the past three decades due to its potential to reduce the cost solar panel. OSC is one of the few emerging solar cell technologies which is evolving to high power conversion efficiency (PCE) required for mass production [1]. Hence, OSCs are expected to contribute towards renewable energy sector with high potential of reducing cost of device production, device light weight, and flexible solar panel [2]. Even though OSCs possess such attractive features but they have drawback in terms of low life time, low stability, low efficiency and prone to oxygen and humidity that limits its penetration in energy market [3]. The first Photo-voltaic solar cell was fabricated from crystalline silicon in 1950s at the Bell laboratory. Since then the PCE of silicon based solar cell increases and approaching currently the theoretical limit 30% [4]. On the other hand, organic solar cells were introduced around 1990 [5] and the PCE continuously increasing to nearly 20% from single junction non-fullerene based OSC. The efficiency of OSCs remains low relative to other emerging and established solar cell technologies due to the poor charge transport processes in organic medium.

Bulk heterojunction is the most successful design of solar absorber in OSC which creates large donor/accepter molecules interfaces for enhanced exciton dissociation [6]. Furthermore, BHJ is allowing an efficient charge dissociation by reducing recombination processes in the photo-active medium. Consequently, the OSCs research gained significant attention because of continuous growth in PCE. However, fullerene based OSC has an efficiency close to 14% because of poor energy band tunability and optical absorption [7]. One of the challenges in polymer solar cell is the short diffusion length of the excitons where the thickness of the absorber layer plays a role for charge collections by the electrodes. In this report, we have investigated the effect of ZnS doped hole transport layer and thickness dependence absorber layer on the performance of thin film solar cells. We employed device simulation program known as solar cell capacitance simulator (SCAPS) which is a one-dimensional device simulation program to investigate the effect of changes on the parameters under investigation. The metal nanoparticles in dielectrics medium exhibits a phenomenon called Local Surface Plasmon Resonance (LSPR) due to the interaction with incident electromagnetic radiation. The excitation of LSPR de-phases through a number of channels including, generation of hot electrons, near field enhancement, charge transfer, energy transfer and light trapping through scattering [8–10]. This investigation takes into account of the advantages of metal nanoparticles on improving charge dissociation and light trapping processes in the functional layers of the solar cell. The article is composed of background theory of metal plasmon, device simulation and discussion of the results.

*E-mail me at: mola@ukzn.ac.za

II. LOCALIZED SURFACE PLASMON RESONANCE

The interaction between the incident electromagnetic (EM) radiation and metal nanoparticle in dielectric medium leads to the polarization of the surface charge on the metal nano-particles resulting in the excitation of surface charge plasmon resonances. Figure 1a depicts the electric field component of EM field displaced the surface electron plasma of the metal to one direction creating a dipole moment the oscillate with the frequency of the incident radiation. This oscillation stores energy that dephase in the form generating hot electron or other forms energy transfer. The occurrence of LSPR is dependent on the size, shape, position, and the geometry of nanomaterial [11–14].

The generation of hot electrons exhibited in the form optical absorption whose absorbance can be expressed in terms of Mie theory of classical electromagnetic light scattering. The absorption and scattering cross section are given by [11].

$$C_{abs} = \frac{2\pi}{\lambda} Im[\alpha] \,, \tag{1}$$

and,

$$C_{scatt} = \frac{1}{6\pi}\left(\frac{2\pi}{\lambda}\right)^4 |\alpha|^2 \,. \tag{2}$$

Where λ is the electromagnetic field wavelength, and α is the polarizability of the particle which is given by

$$\alpha = 3V\frac{\omega_p^2}{\omega_p^2 - 3\omega - i\gamma\omega} = 3V\left[\frac{\varepsilon_p/\varepsilon_m - 1}{\varepsilon_p/\varepsilon_m + 2}\right] \,, \tag{3}$$

where V is the particle volume, ε_p is the dielectric function of the particle and ε_m is the dielectric function of the embedding medium.

The excited electrons are sometimes referred as the hot-electrons. These generated hot-electrons will be available for photo-generated current in semi-conductors Figure1b. Another forms of dephasing the LSPR excitation is the formation near field which scattered light from the nanoparticles into the medium [14]. The scattering of light in the vicinity of the semi-conductor is a necessity to increase optical pathlength of the light in the medium. This is a processes in which light scatters multiple times within or near the semi-conductor such that the light remain longer in the semi-conductor medium until it is efficiently absorbed by the material.

III. DEVICE PREPARATION AND NUMERICAL SIMULATION

Organic solar cell is composed of layers of different materials for different roles to be played in the function of the solar cell. The schematic representation of the solar cell structure provided in Figure 2 consists of various layers of materials at different thickness. The device simulation program SCAPS is a one dimensional simulation programme developed at the department of Electronics and Information Systems (ELIS) of the University of Gent, Belgium by a group of researchers listed in references [15–18]. The structure of the real OSC devices are represented by Schematic diagram (Figure 2), which consists is analogues to real devices fabricated in the experiment where an electrode is added on the substrate followed by the buffer layer then the active layer and lastly another buffer layer and the electrode. The device simulation follows the same structure The materials were added as follows: Indium Tin Oxide (ITo), poly(3,4-ethylenedioxythiophene) polystyrene sulfonate (PEDOT:PSS), The poly(3-hexylthiophene) : [6,6]-phenyl C61-butyric acid methylester (P3HT:PCBM), Lithium Fluoride (LiF),Aluminium (Al).

The material parameters used for the P3HT:PCBM and ZnS layers are shown in Table 1. Where ref 1 and ref 2 are the references of parameters used for P3HT:PCBM and ZnS Np respectively.

The SCAPS simulator numerically solves the set of one-dimensional semi-conductor equations, by firstly discretizing them and uses the Gummel iteration method and Newtons Raphson to solve these equations. Within the bulk of the layers these equations are given by [17**?**]

$$\frac{\partial}{\partial x}(\varepsilon\frac{\partial\psi}{\partial x}) = -\frac{q}{\varepsilon_0}\left[-n + p - N_A^- + N_D^+ + \frac{\rho_{def(n,p)}}{q}\right] \,, \tag{4}$$

$$-\frac{\partial J_n}{\partial x} + G - U_n = \frac{\partial n}{\partial t} \,, \tag{5}$$

$$-\frac{\partial J_p}{\partial x} + G - U_p = \frac{\partial p}{\partial t} \,. \tag{6}$$

Along with the following constitutive equations

$$J_n = -\frac{\mu_n n}{q}\frac{\partial E_{F_n}}{\partial x} \tag{7}$$

$$J_p = -\frac{\mu_p P}{q}\frac{\partial E_{F_p}}{\partial x} \,. \tag{8}$$

In this set of equations n and p have been used to denote the free carrier concentrations. $-N_A^-$ and N_D^+ represent the charged dopant's. ρ_{def} is the defect distribution. The electron and hole current densities and denoted by J_n and J_p respectively. The net recombination rates given by U_n and U_p, while the generation rate is given by G. The generation rate may be calculated using the following set of equations [7, 8, 18]

$$G(x,\lambda) = \frac{1}{2}c\epsilon\alpha n|E(x)|^2 \tag{9}$$

$$\tag{10}$$

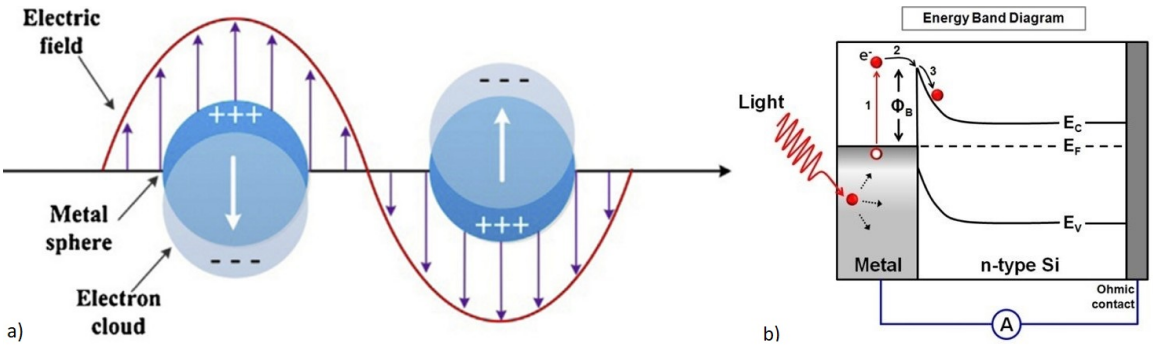

FIG. 1: a) The schematic diagram of LSPR [35], b) Generation of electrons, injection of hot electrons into conduction band of the semiconductor[15]

TABLE I: P3HT:PCBM and ZnS NPs simulation parameters

parameter & symbol & P3HT:PCBM & ZnS Nps & units & ref$_1$ & ref$_2$						
Thickness	d	variable	variable	nm		
Energy band gap	E_g	1.8	3.5	eV		[19–21]
Electron affinity	χ	3.8	3.8	e V	[22]	
Di-electric permittivity(relative)	ϵ	3.8	10		[22]	
CB effective density of states	N_C	1×10^{19}	1×10^{19}	cm^{-3}	[23]	
VB effective density of states	N_V	1×10^{19}	1×10^{19}	cm^{-3}	[23]	
electron thermal velocity	v	1×10^7	1×10^7	$cm\,s^{-1}$		
hole thermal velocity	v	1×10^7	1×10^7	$cm\,s^{-1}$		
electron mobility	μ_n	0.001	160	cm^2/Vs	[21]	[25]
hole mobility	μ_p	0.001	5	cm^2/Vs	[21]	[25]
doping concentration of acceptors	N_A	0	0	cm^{-3}	[22]	
doping concentration of Donors	N_D	0	1×10^{14}	cm^{-3}	[22]	

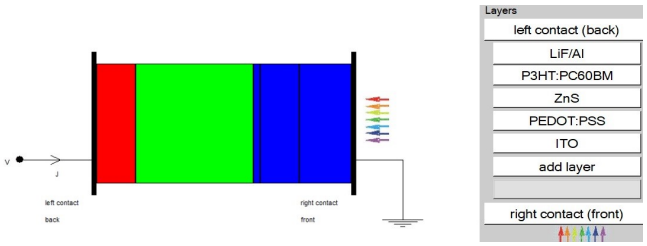

FIG. 2: The conventional solar cell structure in SCAPS

$$G(x,\lambda) = \frac{\lambda Q(z,\lambda)}{hc} \tag{11}$$

$$\tag{12}$$

$$G(\lambda) \quad = \int_{1.5G} Q(x,\lambda)d\lambda \tag{13}$$

Where c is the speed of light, α is the absorption coefficient, and Q represents the energy dissipation.

IV. DEVICE SIMULATION RESULTS

A. P3HT:PCBM Simulation Results

After all parameters were defined, the simulation was then conducted with the light spectrum of $1000\,W\,m^{-2}$ turned on. The simulation was conducted to investigate the effect of varying the thickness of the active layer. A number of device simulations were conducted in this investigation using P3HT:PCBM solar absorber layer in the design of the solar cell. The absorber thickness were varied to study the effect on the device performances.The following results were achieved using the SCAPS programme performed under A.M 1.5G illumination.Figure 3 the J-V curves with the thickness ranging from 120 nm to 300 nm. The main solar cell parameters results found from the device simulation are provided in table2, These results agree with the the experimental results found in reference [26]. According to the results given in Figure 3, the photocurrent found from the device with absorber thickness $120nm$ was lower than the other devices. Which is in fact generated the least power conversion efficiency (see Table 2). But, as the thickness increases the power conversion efficiency

also increases because of the enhanced photocurrent. The maximum power conversion efficiency was found at an absorber layer thickness 200nm as shown in Figure 3. This variations of absorber layer thickness in the devices basically affected almost all device parameters such as Jsc, FF and PCE. The highest performance of

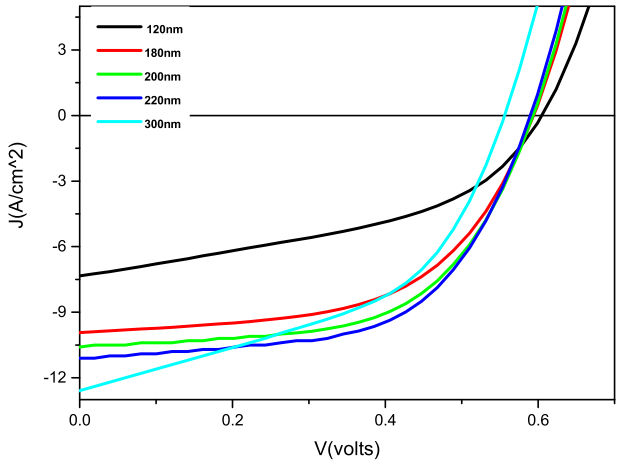

FIG. 3: The J-V curves of P3HT:PCBM at different thickness

P3HT:PCBM is observed at the thickness ranging from 180 nm to 220 nm, The FF is about 48 % at the thickness of 120 nm and 52 % at the thickness of 220 nm (Figure 4). The short current density increases from 7.336 mA cm^{-2} at the thickness of 120 nm to 10.89 mA cm^{-2} at the thickness of 220 nm. This improvement is due to the increased photons absorption which resulted in enhanced photo-generated current. Figure 4 shows the variations

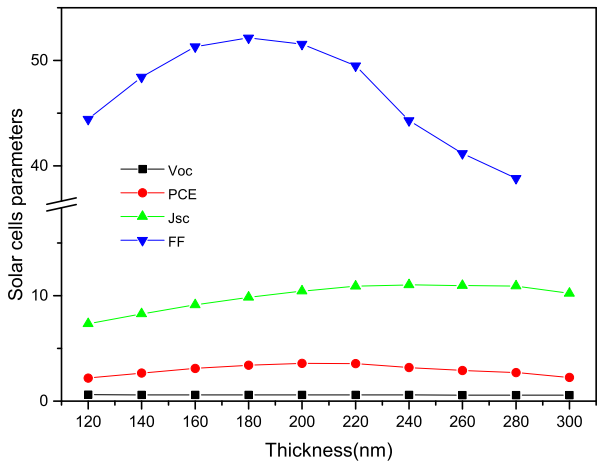

FIG. 4: The solar cell characterization parameters plotted against absorption of the increased photon

of the solar cell parameters with thickness from 120 nm-300 nm. The device parameters increase to a maximum values near the thickness from 180 nm to 220 nm.The V_{oc} remained at a constant [27], [28] range of 0.5615 V -0.6052 V for both simulated and experimental results. And this is because theV_{oc} is mostly dominated by the difference in energy of lowest unoccupied molecula orbital (LUMO) of the acceptor material and the energy of the Highest occupied molecular orbital(HOMO) of the donor material [28],and the work function of the electrode. However visible changes are observed at large thickness $>$ 220 nm. The power conversion efficiency is increasing from 2.19 % to 3.57 % at 120 nm to 220 nm. In similar thickness range All parameters are decreasing as the thickness increases beyond 220 nm, including the V_{oc} , which confirmed by device simulation results(table2). The the V_{oc} decreases from 0.5925 V to 0.562 27 V. The J_{sc} decreases from 10.90 mA cm^{-2} to 10.21 mA cm^{-2}. The Fill Factor drops from 52 % to 35 %. The factors which affect these parameters are series resistance and shunt resistance of the devices.The Shunt resistance prevent the leakage through the current pathways. The shunt resistance decreases with increasing thickness while the series resistance increases with thickness [29] because polymer medium become more resistance to current flow as the in thick polymer medium. The FF increases with increasing shunt resistance and decreasing series resistance. But, while increasing thickness means high the series resistance which reduces the value of the FF. According to the observation of this study,A slight increase in a series resistance has no impact on the short current density, unless it increases drastically.The short current density is also affected by generation, recombination rate and built in electric field [28]. As it can be seen from Poisson's continuity equation 7 and 8,The solution of the current $J(v)$ explicitly depends on the recombination and generation coefficient,Large thickness results in the recombination(since the exciton diffusion length is short) [28] of carriers thus carriers lose energy in the form of heat. Increasing thickness decreases the built in electric field, which therefore leads to an excitton dissociation failure, since the exciton is separated by the electric field in donor-acceptor interface[28]. Figure5 is the quantum efficiency, which is defined as the number of collected charge carriers divide by the number of incident photons.

About 80 % of charge carriers are collected when the active layer has thickness of 120 nm,For 220 nm, about 90 % of charge carriers are collected, and lastly for 300 nm about 95 % of charge carriers are collected.

B. Capacitance Voltage Plot Results

The depletion region known as the space charge is the result of the potential barrier created: between a semi-

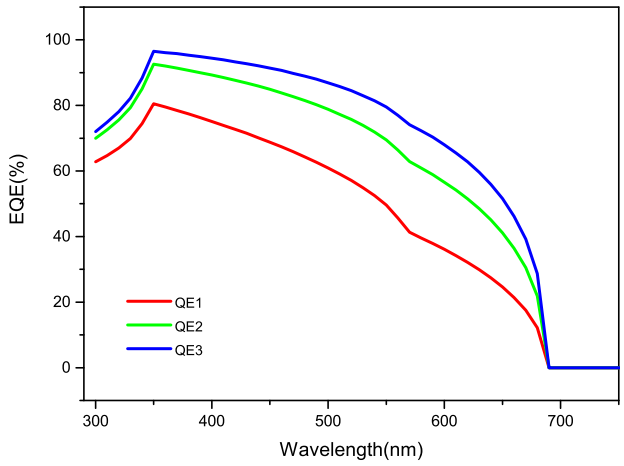

FIG. 5: The External Quantum Efficiency plotted against the thickness

TABLE II: p3ht:pcbm characteristics parameters simulation results

Thickness	V_{oc}/V	$J_{sc}/mA/cm^2$	FF/%	η/%
120	0.6051	7.3366	44,43	2.19
180	0.5959	9.8484	52.13	3.40
200	0.5955	10.437	51.54	3.57
220	0.9525	10.895	49.49	3.55
300	0.5621	10.214	35.30	2.25

conductor material and the metal, or in the junction of the p-type and n-type material. The p-n junction is formed when an n-type material and p-type material are brought together, which can result in the diffusion of carriers occurring when there is a large carrier concentration gradient at the junction. This carrier diffusion is caused by thermal energy since there is no external field. On the other hand, the potential gradient is created across the p-n junction which results in the creation of a drift current which is the counterpart of the diffusion current. Under equilibrium conditions, the net current at the space charge is zero [30]. Any carriers present in the depletion region can only exist due to doping (defects) [32]. The space charge introduces capacitance (Capacitance is responsible for charge storage), which is very useful in solar cells. A capacitance is large in a forward bias solar cell because the space charge region is increased, and small in a reverse bias solar cell because the space charge region is increased [31]. The information extracted from capacitance is Its response to applied voltage or frequency, The values for parameters like built-in potential and doping density (in C-V plots).The capacitance is given by equation 12 [32]

$$C = \frac{\varepsilon_0 \varepsilon_r A}{w} \tag{14}$$

Where ε_0 and ε_r are the permittivity of free space and the relative dielectric constant of a doped material. w is the width depletion, which is given by equation 13.

$$w = \sqrt{\frac{2\varepsilon_0 \varepsilon_r (V_{bi} - V)}{qN}} \tag{15}$$

Where V_{bi} is built in voltage, V is bias voltage, q is the elementary charge ,and N is the doping concentration given in equation 14 [31].

$$N = \frac{N_A N_D}{N_A + N_D} \tag{16}$$

N_A and N_D being the the doping concentration of p and n regions respectively. The inverse square of the capacitance gives a linear relationship with the voltage [32],This inverse square of capacitance is refered as the Mott Schottky which is given by equation 15 [33]. It's slope is used to find the doping concentration and the x-intercept is used to find the built in voltage [32]. In many literatures, it is reported that the CV and Mott Schottky plot can result in inaccurate values of the built in potential and the doping density.

$$C^{-2} = \frac{2(V_{bi} - V)}{\varepsilon_0 \varepsilon_r A^2 q N} \tag{17}$$

The capacitance is high at low thickness due to small depletion width. The increased thickness increases the depletion region which results in charge recombination hence the capacitance is reduced as shown in figure 6 and equation 13.
The Mott Schottky plot is shown in Figure7, We selected the graph of 180 nm thickness(Figure8) to extract the built in potential. The straght line was fitted on the same set of axis. The x-intercept of this straight line is the built in potential which was found to be $V_{bi} = 0.5$ V.

C. ZnS Nps Simulation results

We kept 180 nm active layer thickness to investigate the effect of incorporating ZnS Nps in OSC devices. The ZnS Nps were chosen because of their broad application in different areas. They are commonly used in optoelectronic devices such as blue lighting emitting diodes, solar cells and field emission devices [34]. Many studies focus on varying the Nps weight, either added in the active layer or in the buffer layer. In this study, we

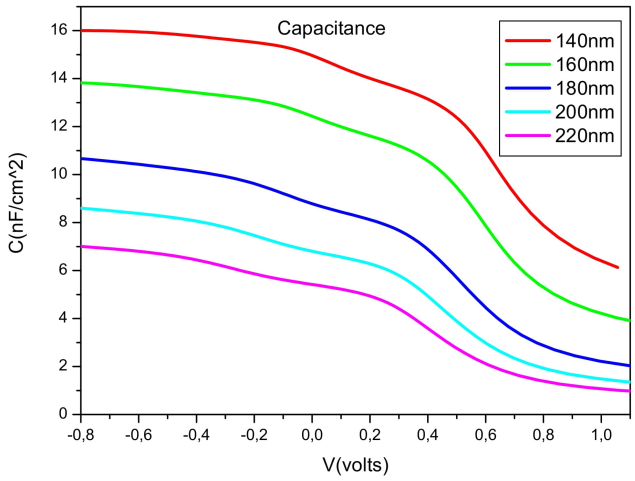

FIG. 6: The capacitance voltage plot of the Pristine with the thickness varied from 140 nm to 220 nm

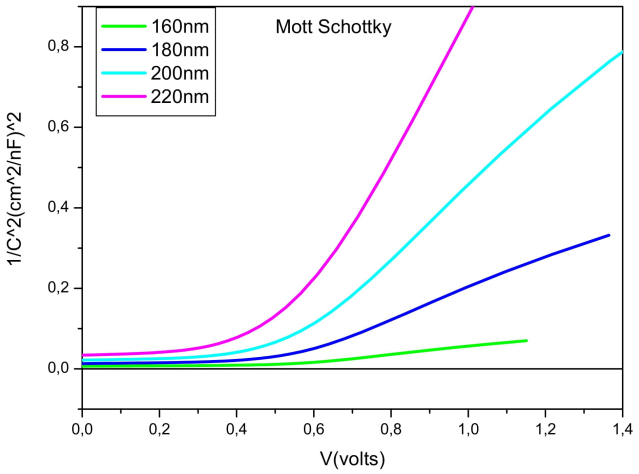

FIG. 7: The Mott Schottky plot of the Pristine with the thickness varied from 160 nm to 220 nm

chose to investigate the thickness of the ZnS nanoparticles incorporated as a core layer between the active layer (P3HT:PCBM) and buffer layer(PEDOT:PSS). The ZnS thickness was varied from 3 nm to 12 nm.The best performance is observed at the thickness of 3 nm, The efficiency reaches the maximum value of 4.06 %, The FF = 61.56 %, Jsc = 10.24 mA cm^{-2}, and the Voc = 0.5800 V (as shown in figure9, Figure 11 , and Table3). This performance is much better than that of Pristine, This shows that there is improvement in both absorption and collection of charges. There is huge improvement in the efficiency and Fill factor, The FF vary drastically with the thickness of ZnS Np. The FF is given by the following equation

$$FF = \frac{P_{max}}{V_{oc} J_{sc}} \tag{18}$$

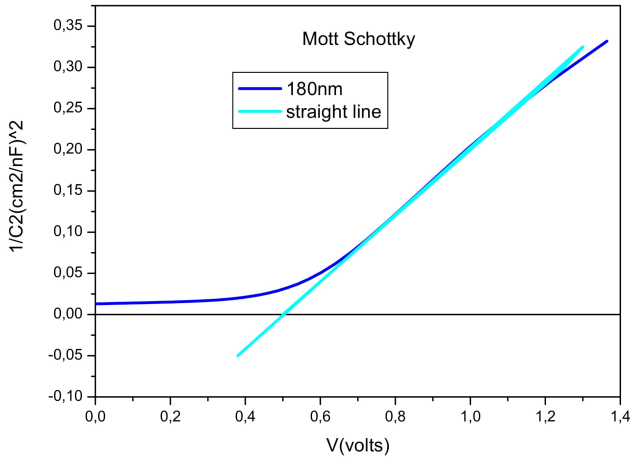

FIG. 8: The Mott Schocttky plot of the Pristine with the thickness of 180 nm and a fitted straight line on it

On this equation the FF strongly depends on the maximum power, the maximum power which is given by the product of V_{max} and J_{max}. From Figure5 the 3 nm, has the highest maximum power compared to other curves(9 nm to 12 nm). hence the FF is high at 3 nm. According to device simulation results the solar cell pa-

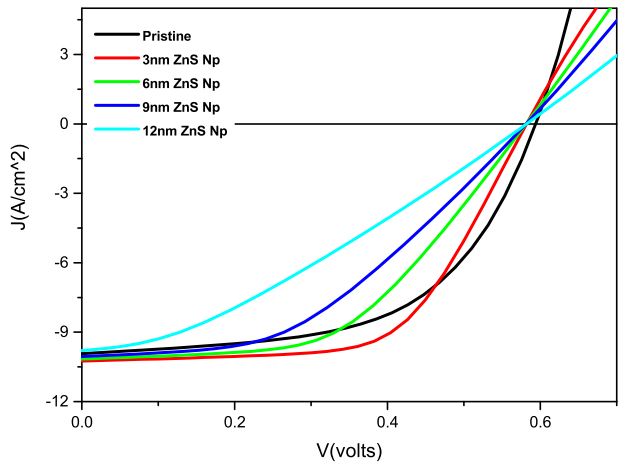

FIG. 9: The J-V curves of P3HT:PCBM + ZnS Nps at different thickness of ZnS Nps

rameters such as Jsc and FF and efficiency decrease with an increasing thickness of the ZnS Nps(see Figure11 and Table3). From this study we observed that it is hard to improve the Jsc by increasing the ZnS Np thickness(beyond 6nm) especially when the band gap of the core layer is beyond 2.5 eV. The short current density is almost the same in each ZnS thickness value. It has been observed in many experiment, that the large weight of Nps result in poor performing devices. Increasing the concentration

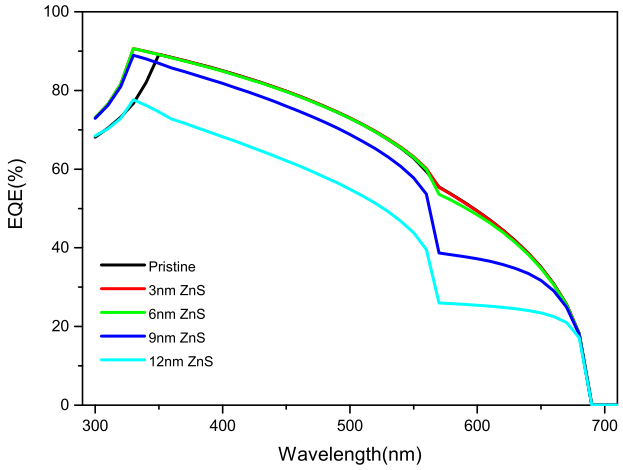

FIG. 10: The External Quantum efficiency plotted against the ZnS Np thickness

of Nanoparticles increases the defects in a device material.The defects can poorly affect the photon absorption by device material. Defects also result in the recombination of charges.The increasing Np thickness increases the Series resistance and lowers the shunt resistance, which limits the maximum power. We ploted the quantum efficiency graph shown in Figure 10. The External quantum

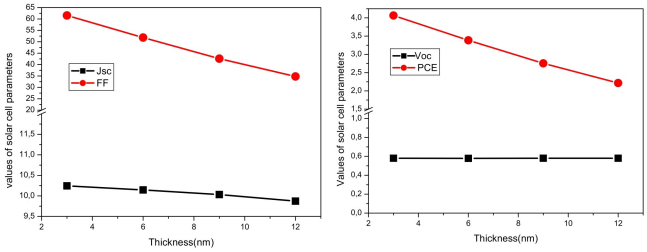

FIG. 11: The solar cell characterization parameters plotted against ZnS Np thickness

efficiency is about 90% when the ZnS Np has a thickness of 3nm. The EQE decreases with increasing thickness. The large band gap of ZnS Nps influenced both absorption and collection of charges, The are observable changes in EQE graph especially at the wavelength of 570 nm, the EQE drops drastically as the ZnS thickness is increasing from 9 nm to 12 nm(Figure11). This shows that the light of large wavelength is partially absorbed by the Nanoparticle, most of it is transmitted. Even the high energetic photons are less absorbed when the the ZnS Np has the thickness of 12 nm. The EQE drops to about 80 % as the thickness is increased from 9 nm to 12 nm.

TABLE III: p3ht:pcbm + ZnS solar characteristics parameters results table

Thickness/nm	V_{oc}/V	$J_{sc}/mA/cm^2$	FF/%	η/%
pristine	0.5959	9.8484	52.13	3,40
3	0.5800	10.244	61.56	4.06
6	0.5790	10.146	51.87	3.39
9	0.5799	10.033	42.59	2.75
12	0.5804	9.8725	34.79	2.22

V. CONCLUSION

With the aid of the simulation device programme, appreciable results were obtained from the study of absorber layer thickness dependence of the performance of OSC. The results found from the investigation are comparable to experimental results reported from the same absorber layer (P3HT:PCBM). The simulation was carried out using the illumination of 1.5G spectrum.The device programme works under room temperatures, allows single or batch calculations at once. The thickness of active layer was varied and the parameters that characterize the solar cell were observed with thickness. According to device simulation results the peak efficiency was observed from 180 nm to 220 nm,The improvement in device performance with absorber thickness associated with enhanced light absorption that generated more photocurrent.The highest efficiency achieved in this study was 3.57 %, which agrees with the experimental results and in literatures. The best device performance and parameters were found at the thickness ranging from 180 nm to 220 nm. Beyond this range all the device parameters drop and device performance are also reduced. And the Series resistant, Shunt resistance and recombination of carries were assumed to be the main factors contributed to this poor performance of cell at thickness approaching 300 nm. Generally, all the solar cell parameters demonstrated that they are affected by the active layer thickness. Therefore, the thickness of active layer play an important role in designing OSC devices. We also employed the ZnS nano-particles, to increase the performance and improve the conductivity of holes in the device. The maximum efficiency of 4.06 % at the thickness of 3 nm of ZnS Nps was achieved. Much enhancement was observed on the FF other than other solar parameters.These results serve as a guidance on how ZnS NPs can be used as a hole transport material, in improving the conductivity between the PEDOT:PSS and P3HT:PCBM, and also enhancing the light absorption. It can also be used as acceptor material due to it's high electron affinity which can assisst in exciton dissociation, and large electron mobility which improves the conductivity of electrons between the active layer(P3HT:PCBM) and buffer layer(LiF).

Declaration of competing interest

The authors declare that they have not known any competing financial interests or personal relationships that could have influenced the work reported in this paper.

Acknowledgments

This work is supported by the National Research Foundation (NRF) (Grant Nos., 85589, 113831), South Africa. The authors also appreciate the Microscopy and Microanalysis Unit (MMU) staff at UKZN for several SEM and TEM measurements.

[1] Abdulrazzaq, O.A., Saini, V., Bourdo, S., Dervishi, E. and Biris, A.S.,2013. Organic solar cells: a review of materials, limitations, andpossibilities for improvement. Particulate science and technology, 31(5), pp.427-442.

[2] Samanta, M., Chattopadhyay, K.K. and Bose, C., 2018, November. A Simulation Based Comparative Study of P3HT: PCBM and OC 1 C 10 PPV: PCBM Organic Solar Cells. In 2018 IEEE Electron Devices Kolkata Conference (EDKCON) (pp. 218-221). IEEE.

[3] Clare Dyer-Smith, Jenny Nelson (2012).Chapter IE-2 - Organic Solar Cells. Practical Handbook of Photovoltaics (SecondEdition),volume(issue), pp-543-569

[4] Blom, P.W., Mihailetchi, V.D., Koster, L.J.A. and Markov, D.E., 2007. Device physics of polymer: fullerene bulk heterojunction solar cells. Advanced Materials, 19(12), pp.1551-1566.

[5] Karagiannidis, P.G., Kalfagiannis, N., Georgiou, D., Laskarakis, A., Hastas, N.A., Pitsalidis, C. and Logothetidis, S., 2012. Effects of buffer layer properties and annealing process on bulk heterojunction morphology and organic solar cell performance. Journal of Materials Chemistry, 22(29), pp.14624-14632.

[6] Scharber, M.C. and Sariciftci, N.S., 2013. Efficiency of bulk-heterojunction organic solar cells. Progress in polymer science, 38(12), pp.1929-1940.

[7] Zaidi, B. ed., 2018. Solar Panels and Photovoltaic Materials. BoDBooks on Demand.

[8] Dlamini, M.W. and Mola, G.T., 2019. Near-field enhanced performance of organic photovoltaic cells. Physica B: Condensed Matter, 552, pp.78-83.

[9] Hamed, M.S.G. Oseni,S.O. Kumar,A. Sharma,G. Mola,G.T., 2020. Nickel sulphide nano-composite assisted hole transport in thin film polymer solar cells, Solar Energy, 195, pp.310-317

[10] Mola,G.T. Arbab,E.A.A. Taleatu, E.A. Kaviyarasu, K. Ahmad I. and M. Maaza, 2017. Growth and characterization of V2O5 thin film on conductive electrode, J. Microscopy, Vol. 265 (2), pp. 214-221

[11] Notarianni, M., Vernon, K., Chou, A., Aljada, M., Liu, J. and Motta, N., 2014. Plasmonic effect of gold nanoparticles in organic solar cells. Solar Energy, 106, pp.23-37.

[12] Kalfagiannis, N., Karagiannidis, P.G., Pitsalidis, C., Panagiotopoulos, N.T., Gravalidis, C., Kassavetis, S., Patsalas, P. and Logothetidis, S., 2012. Plasmonic silver nanoparticles for improved organic solar cells. Solar Energy Materials and Solar Cells, 104, pp.165-174.

[13] Mola, G.T., Mthethwa, M.C., Hamed, M.S., Adedeji, M.A., Mbuyise, X.G., Kumar, A., Sharma, G. and Zang, Y., 2020. Local surface plasmon resonance assisted energy harvesting in thin film organic solar cells. Journal of Alloys and Compounds, 856, p.158172.

[14] Petryayeva, E. and Krull, U.J., 2011. Localized surface plasmon resonance: Nanostructures, bioassays and biosensingA review. Analytica chimica acta, 706(1), pp.8-24.

[15] Lin, K.T., Lin, H. and Jia, B., 2020. Plasmonic nanostructures in photodetection, energy conversion and beyond. Nanophotonics, 9(10), pp.3135-3163.

[16] Boriskina, S.V., Ghasemi, H. and Chen, G., 2013. Plasmonic materials for energy: From physics to applications. Materials Today, 16(10), pp.375-386.

[17] Burgelman, M., Decock, K., Niemegeers, A., Verschraegen, J. and Degrave, S., 2016. SCAPS manual. February.

[18] Minbashi, M., Ghobadi, A., Ehsani, M.H., Dizaji, H.R. and Memarian, N., 2018. Simulation of high efficiency SnS-based solar cells with SCAPS. solar energy, 176, pp.520-525.

[19] KROON, R., LENES, M., HUMMELEN, J.C., BLOM, P.W. and DE BOER, B.E.R.T., 2008. Small Bandgap Polymers for Organic Solar Cells (Polymer Material Development in the Last 5 Years). Polymer Reviews, 48, pp.531-582.

[20] Oyedele, S.O. and Aka, B., 2017. Numerical simulation of varied buffer layer of solar cells based on cigs. Modeling and Numerical Simulation of Material Science, 7(03), p.33.

[21] Khelifi, S., Voroshazi, E., Spoltore, D., Piersimoni, F., Bertho, S., Aernouts, T., Manca, J., Lauwaert, J., Vrielinck, H. and Burgelman, M., 2014. Effect of light induced degradation on electrical transport and charge extraction in polythiophene: Fullerene (P3HT: PCBM) solar cells. Solar energy materials and solar cells, 120, pp.244-252.

[22] Omer, B.M., 2015. Effect of Valence Band Tail Width on the Open Circuit Voltage of P3HT: PCBM Bulk Heterojunction Solar Cell: AMPS-1D Simulation Study.

[23] Khalid, S., Voroshazi, E., Spoltore, D., Piersimoni, F., Bertho, S., Aernouts, T., Manca, J., Lauwaert, J., Vrielinck, H. and Burgelman, M., 2014. Effect of light

induced degradation on electrical transport and charge extraction in polythiophene: Fullerene (P3HT: PCBM) solar cells. Solar energy materials and solar cells, 120, pp.244-252.

[24] Nadeem, M.Y. and Ahmed, W., 2000. Optical properties of ZnS thin films. Turkish Journal of Physics, 24(5), pp.651-659.

[25] Huang, S.C., Lin, J.T., Haga, S., Chen, W.H. and Ho, K.Y., 2018, October. A Three-Terminal ZnS-based CIGS Solar Cell. In 2018 14th IEEE International Conference on Solid-State and Integrated Circuit Technology (ICSICT) (pp. 1-3). IEEE.

[26] Jin, H., Olkkonen, J., Tuomikoski, M., Kopola, P., Maaninen, A. and Hast, J., 2010. Thickness dependence and solution-degradation effect in poly (3-hexylthiophene): phenyl-C61-butyric acid methyl ester based solar cells. Solar Energy Materials and Solar Cells, 94(3), pp.465-470.

[27] Lee, D., Kim, J., Noh, S. and Lee, C., 2010, August. The thickness of active layer dependence of polymer solar cells. In 10th IEEE International Conference on Nanotechnology (pp. 1175-1178). IEEE.

[28] Nam, Y.M., Huh, J. and Jo, W.H., 2010. Optimization of thickness and morphology of active layer for high performance of bulk-heterojunction organic solar cells. Solar Energy Materials and Solar Cells, 94(6), pp.1118-1124.

[29] Samanta, M., Chattopadhyay, K.K. and Bose, C., 2018, November. A Simulation Based Comparative Study of P3HT: PCBM and OC 1 C 10 PPV: PCBM Organic Solar Cells. In 2018 IEEE Electron Devices Kolkata Conference (EDKCON) (pp. 218-221). IEEE.

[30] Zekry, A., Shaker, A. and Salem, M., 2018. Solar cells and arrays: principles, analysis, and design. In Advances in renewable energies and power technologies (pp. 3-56). Elsevier.

[31] Kirchartz, T., Gong, W., Hawks, S.A., Agostinelli, T., MacKenzie, R.C., Yang, Y. and Nelson, J., 2012. Sensitivity of the MottSchottky analysis in organic solar cells. The Journal of Physical Chemistry C, 116(14), pp.7672-7680.

[32] Fabregat-Santiago, F., Garcia-Belmonte, G., Mora-Ser, I. and Bisquert, J., 2011. Characterization of nanostructured hybrid and organic solar cells by impedance spectroscopy. Physical chemistry chemical physics, 13(20), pp.9083-9118.

[33] Willis, S.M., Cheng, C., Assender, H.E. and Watt, A.A., 2011. Modified Mott-Schottky Analysis of Nanocrystal Solar Cells. arXiv preprint arXiv:1112.1623.

[34] Mehta, S.K., Kumar, S., Chaudhary, S., Bhasin, K.K. and Gradzielski, M., 2009. Evolution of ZnS nanoparticles via facile CTAB aqueous micellar solution route: a study on controlling parameters. Nanoscale research letters, 4, pp.17-28.

[35] Cao, J., Sun, T. and Grattan, K.T., 2014. Gold nanorod-based localized surface plasmon resonance biosensors: A review. Sensors and actuators B: Chemical, 195, pp.332-351.

Highlights

- ZnS nano-particle is an effective mechanism to improve charge transport process in polymer solar cell.
- The use of nano-particles improved the collection of photo-current.
- ZnS can reduce charge recombination at the metal/polymer interfaces.

Declaration of interests

☒The authors declare that they have no known competing financial interests or personal relationships that could have appeared to influence the work reported in this paper.

☐The authors declare the following financial interests/personal relationships which may be considered as potential competing interests: